Applied Catalysis A, General 599 (2020) 117569

Contents lists available at ScienceDirect

Applied Catalysis A, General

journal homepage: www.elsevier.com/locate/apcata

Efficient oxidation of p-xylene to terephthalic acid by using N,N-dihydroxypyromellitimide in conjunction with Co-benzenetricarboxylate

Luo Xu[a], Dawei Chen[a], Haoran Jiang[a], Xia Yuan[a,b,*]

[a] College of Chemical Engineering, Xiangtan University, Xiangtan, 411105, China
[b] National & Local United Engineering Research Centre for Chemical Process Simulation and Intensification, Xiangtan, 411105, China

ARTICLE INFO

Keywords:
p-Xylene oxidation
Terephthalic acid
Co-benzenetricarboxylate
NDHPI
Metal–organic framework

ABSTRACT

The MOF Co-BTC (BTC = benzenetricarboxylate) has been synthesized by a hydrothermal method, and characterized by means of N_2 physical adsorption, X-ray diffraction, scanning electron microscope, thermogravimetric analysis, and X-ray photoelectron spectroscopy. The material has multiple crevices, as opposed to a pore structure, and shows high thermal stability, with Co in the divalent state. It has been used in conjunction with *N,N*-dihydroxypyromellitimide to catalyze the oxidation of *p*-xylene to terephthalic acid, the reaction conditions for which have been investigated and optimized. At 150 °C, with acetonitrile as solvent instead of acetic acid and in the absence of corrosive bromine, the conversion of *p*-xylene reached 100 % and the selectivity for terephthalic acid exceeded 97 %. Under the optimized conditions, Co-BTC exhibits stronger catalytic activity than cobalt(II) acetate, and maintains excellent stability during the reaction. The reaction mechanism has been deduced, and the roles of *N,N*-dihydroxypyromellitimide and Co-BTC as synergistic catalysts in the reaction have been clarified.

1. Introduction

In the polyester industry, terephthalic acid (TA) is an important raw material used primarily in the manufacture of non-toxic polyethylene terephthalate (PET), which accounts for about 20 % of the polyester market. PET is mainly used in machinery parts, fiber materials, and packaging for foods and medicines.

Oxidation of *p*-xylene (PX) is the main route for obtaining TA. This process is shown in Scheme 1, and is consistent with a mechanism of hydrocarbon radical oxidation. In general, the difficulty of hydrocarbon oxidation lies mainly in the initiation step, that is, the formation of hydrocarbon radicals by the removal of hydrogen from alkyl groups [1–4]. However, in the oxidation of PX, *p*-methyl benzyl radical and *p*-TA will also be present [5], which are resistant to oxidation. Due to the difficult oxidation characteristics of PX, current industrial production of TA mainly relies on the harsh Amoco process, using cobalt(II) acetate, manganese(II) acetate, and bromine as catalysts, and acetic acid as solvent, which is conducted at high temperature (about 200 °C) and high pressure (1.5–3.0 MPa). The selectivity for TA is over 95 %. Under the high-temperature operating conditions, corrosive bromine acts as a co-catalyst, resulting in high production and equipment costs. Therefore, the quest for an efficient and mild catalyzed route for PX oxidation, leading to TA without the need for acid and bromine, has become a hot topic of research.

N-Hydroxyphthalimide (NHPI) and its derivatives are effective catalysts for the oxidation of organic compounds by molecular oxygen under mild conditions [6], and are widely used as initiators for the oxidation of hydrocarbons. Tashiro et al. [7] used NHPI/$Co(OAc)_2$/$Mn(OAc)_2$ as a catalyst and acetic acid as a solvent to oxidize PX at 100 °C. The yield of TA reached 82 % after 14 h of reaction; when the temperature was raised to 150 °C, the yield of TA reached 84 % after 3 h. Koshino et al. found that the PINO formed by the -NO-H cleavage of NHPI is more likely to capture a proton from the alkyl group on the alkyl aromatic hydrocarbon in acetonitrile (MeCN) than in acetic acid; during the oxidation of PX, the effect of *N,N*-dihydroxypyromellitimide (NDHPI) as an initiator is superior to that of NHPI because it bears two -NOH groups [8].

Heterogeneous catalysts have also been used to catalyze the oxidation of PX [9]. Ratnasamy et al. loaded cobalt manganese oxide into a zeolite to catalyze the oxidation of PX at high temperature (473 K) and an air pressure of 550 psi. The conversion of PX was 100 %, and the selectivity for TA was over 98 %, but corrosive bromine was still needed as a co-catalyst to capture hydrogen from the methyl group [10]. Deka et al. prepared porous CeO_2 as a catalyst to catalyze the oxidation of PX to TA. Using only water as a solvent under extremely mild conditions (70 °C, 1 bar O_2), the conversion of PX reached 100 % and the

* Corresponding author at: College of Chemical Engineering, Xiangtan University, Xiangtan, 411105, Hunan, China.
E-mail address: yxiamail@163.com (X. Yuan).

https://doi.org/10.1016/j.apcata.2020.117569
Received 21 December 2019; Received in revised form 6 April 2020; Accepted 14 April 2020
Available online 07 May 2020
0926-860X/

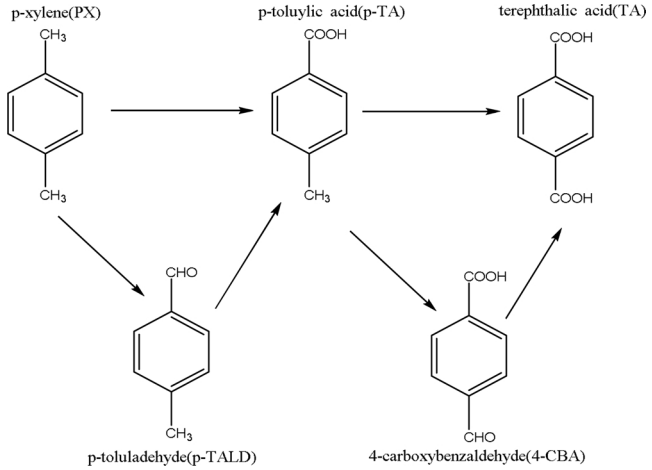

Scheme 1. Oxidation of PX to TA.

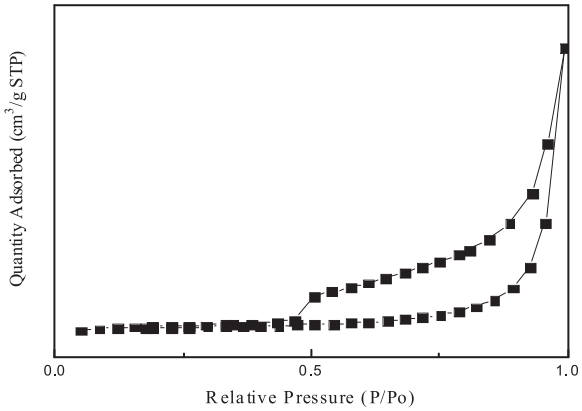

Fig. 1. N_2 adsorption/desorption of Co-BTC.

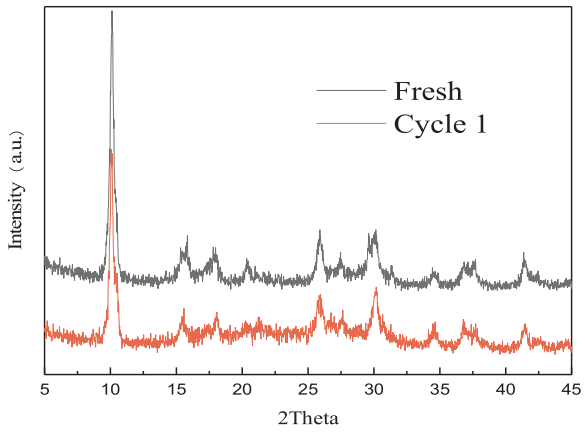

Fig. 2. XRD of Co-BTC.

selectivity for TA exceeded 99 % [11]. Guo et al. used a metalloporphyrin (T(*p*-Cl)PPMnCl) as a catalyst to catalyze the oxidation of PX with acetic acid as a solvent, although its concentration was as high as 20 %. Under these operating conditions (3.5 h, 180 °C, 2.0 MPa), the conversion rate of PX was 41.8 %, the selectivity for *p*-TA is 82.1 %, but the selectivity for TA was only 12.4 % [12].

Porous metal-organic frameworks (MOFs), due to their variable combinations of metals and organic ligands, offer great diversity in their structures and properties, making them suitable for adsorbing drugs [13] and harmful substances [14,15] as well as gas absorption [16–18] and storage [19]. They also have broad prospects and value in

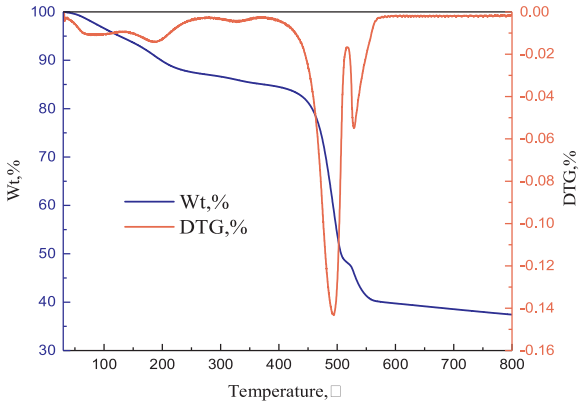

Fig. 3. TGA of Co-BTC.

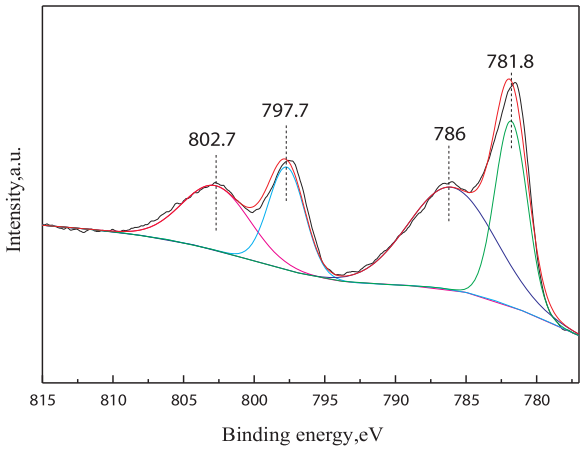

Fig. 4. XPS spectrum of Co-BTC with peak fittings.

the field of catalysis [18,20,19,20,21,22,23]. To date, MOFs have been studied as heterogeneous catalysts in the selective oxidation of some hydrocarbons, such as cyclohexane [24–27], cyclooctane [28], olefins [27,29–32], alcohols, [27,33–35], and so on. Wang et al. used a Cu-MOF as a catalyst to catalyze the oxidation of PX to 4-hydroxymethylbenzoic acid under a mild conditions [36]. To the best of our knowledge, however, no MOFs have hitherto been used in the oxidation of PX to TA.

In this study, Co-BTC (BTC = benzenetricarboxylate) has been used as a catalyst for the first time in the oxidation of PX to TA. It has been used in conjunction with NDHPI instead of corrosive bromine as an initiator for PX oxidation in the non-acidic solvent MeCN. The catalytic properties of Co-BTC and cobalt(II) acetate have also been compared. Through suitably designed experiments, the mode of action of NDHPI and Co-BTC in PX oxidation has been investigated. Furthermore, the stability of Co-BTC in the oxidation of PX has been studied.

2. Materials and methods

2.1. Materials and reagents

MeCN (AR), PX (AR), $Co(OAc)_2{\cdot}4H_2O$ (AR), $Co(NO_3)_2{\cdot}6H_2O$ (AR), trimesic acid (H_3BTC, AR), NDHPI (AR), dimethyl sulfoxide (DMSO, AR), and ethanol (AR) were purchased from Macklin. Water was purified and deionized in our laboratory.

2.2. Synthetic procedure

Co-BTC was synthesized according to a method in the literature [37], with some modifications. The specific process was as follows: Co

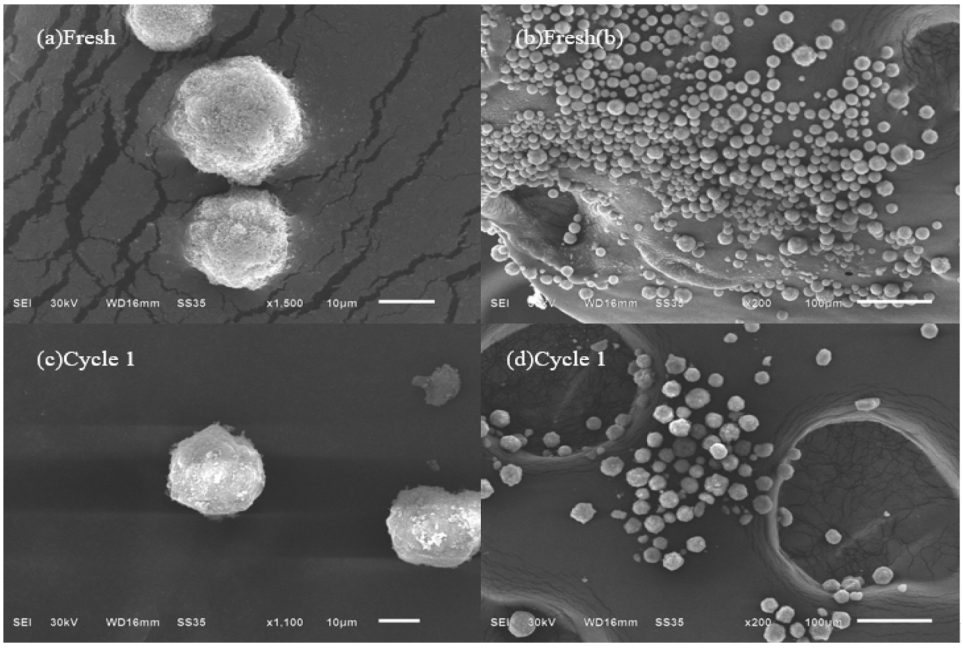

Fig. 5. SEM images of Co-BTC.

Table 1
Study of catalytic performance.

	NDHPI /g	Co-BTC /g	Conversion /%	Selectivity/%			
				p-TALD	*p*-TA	4-CBA	TA
1[a]	0.1	0	0	0	0	0	0
2[a]	0	0.1	0	0	0	0	0
3[a]	0.1	0.1	57.0	3.6	89.4	1.6	5.4
4[b]	0.372	0	93.5	0	30	2.5	67.5
5[b]	0	0.05	3.1	97	3	0	0
6[b]	0.372	0.02	100	0	2.5	1.3	96.2
7[c]	0.372	0	100	0	10	0.9	89.1

[a] Reaction carried out at 100 ℃ for 12 h, 10 g PX, 20 g MeCN, 3.0 MPa O_2.
[b] Reaction carried out at 150 ℃ for 12 h, 0.54 g PX, 25 g MeCN, 3.0 MPa O_2.
[c] Reaction carried out at 150 ℃ for 12 h, 0.54 g PX, 25 g MeCN, 3.0 MPa O_2; 0.025 g $Co(OAc)_2{\cdot}6H_2O$ was added.

$(NO_3)_2{\cdot}6H_2O$ (4.8 g) was dissolved in deionized water (20 mL), and H_3BTC (2.0 g) was dissolved in absolute ethanol (130 mL). When the two materials had completely dissolved, the two solutions were mixed, and the mixture was transferred to a 200 mL Teflon crystallization vessel. After agitation in an ultrasonicator for 20 min, the mixture was transferred to an incubator for crystallization by programmed temperature control. First, the temperature was quickly raised to 140 ˚C within 22 min and maintained at this level for 24 h; it was then uniformly lowered to 120 ˚C in 200 min. After 5 h, the temperature was steadily reduced to 100 ˚C over a period of 200 min and maintained at this level for 5 h. Finally, the mixture was cooled to room temperature. The vessel was removed from the incubator, the supernatant was decanted, and the solid was collected by suction filtration and washed with absolute ethanol until the washings were colorless and transparent. Thereafter, the solid was placed in a vacuum oven at 80 ˚C for 24 h. The dark-blue solid product was designated as Co-BTC.

2.3. Catalysis and product analysis

All reactions were carried out in an autoclave equipped with a 100 mL quartz vessel and operated at a stirring speed of 1000 rpm. In a representative reaction process, combined catalyst (0.372 g NDHPI, 0.05 g Co-BTC), raw material (0.54 g PX), and solvent (25 g acetonitrile) were combined in the quartz vessel. The autoclave was then closed, and the inside of the reactor was flushed twice with oxygen through a valve. The reactor was finally supplied with oxygen (3 MPa, room temperature), then heated to 150 ˚C, and the reaction was allowed to proceed for 12 h. Thereafter, the product was taken up in DMSO and analyzed by high-performance liquid chromatography [38].

2.4. Characterization

The specific surface areas and pore structures of samples were measured by N_2 adsorption using an ASAP 2020 Plus physisorption instrument, whereby the specific surface area was calculated by the Brunauer-Emmett-Teller (BET) method. X-ray diffraction (XRD) analysis was carried out using a Rigaku D/max-2500 X-ray diffractometer employing Cu-K_α radiation at 40 kV and 30 mA. The XRD pattern was recorded in the 2θ range 5 − 45˚. A scanning electron microscope (SEM) image was obtained using an Hitachi S-4800 electron microscope. The thermal stability of the catalyst was measured by thermogravimetric analysis (TGA) using a Netzsch TG209 analyzer. The temperature was raised from ambient to 800 ˚C at 10 ˚C/min under a flow of air/N_2. The chemical state of cobalt was characterized by X-ray photoelectron spectroscopy (XPS).

3. Results and discussion

3.1. Characterization of Co-BTC

Fig. 1 shows the N_2 sorption isotherm of Co-BTC, which features a hysteresis loop of H3 type. This implies that the synthesized Co-BTC had a slit structure. The specific surface area and pore volume were evaluated as 1.9 m^2/g and 0.01 cm^3/g, respectively, indicating that the material had almost no pore structure. Fig. 2 shows the XRD pattern of the synthesized Co-BTC. It features a strong diffraction peak at 10.02˚, which is distinct from the various crystal forms of Co-BTC MOFs reported in the literature [13,37,39–44]. Fig. 3 shows the thermal weight loss trace of Co-BTC, which reveals that the material was relatively stable up to 400 ˚C. Fig. 4 shows the XPS spectrum of cobalt in Co-BTC. The main peaks at 781.8 eV and 797.7 eV can be assigned to Co2p3/2 and Co2p1/2, and the corresponding accompanying peaks are located at 786 eV and 802.7 eV, respectively. Thus, the energy gaps between

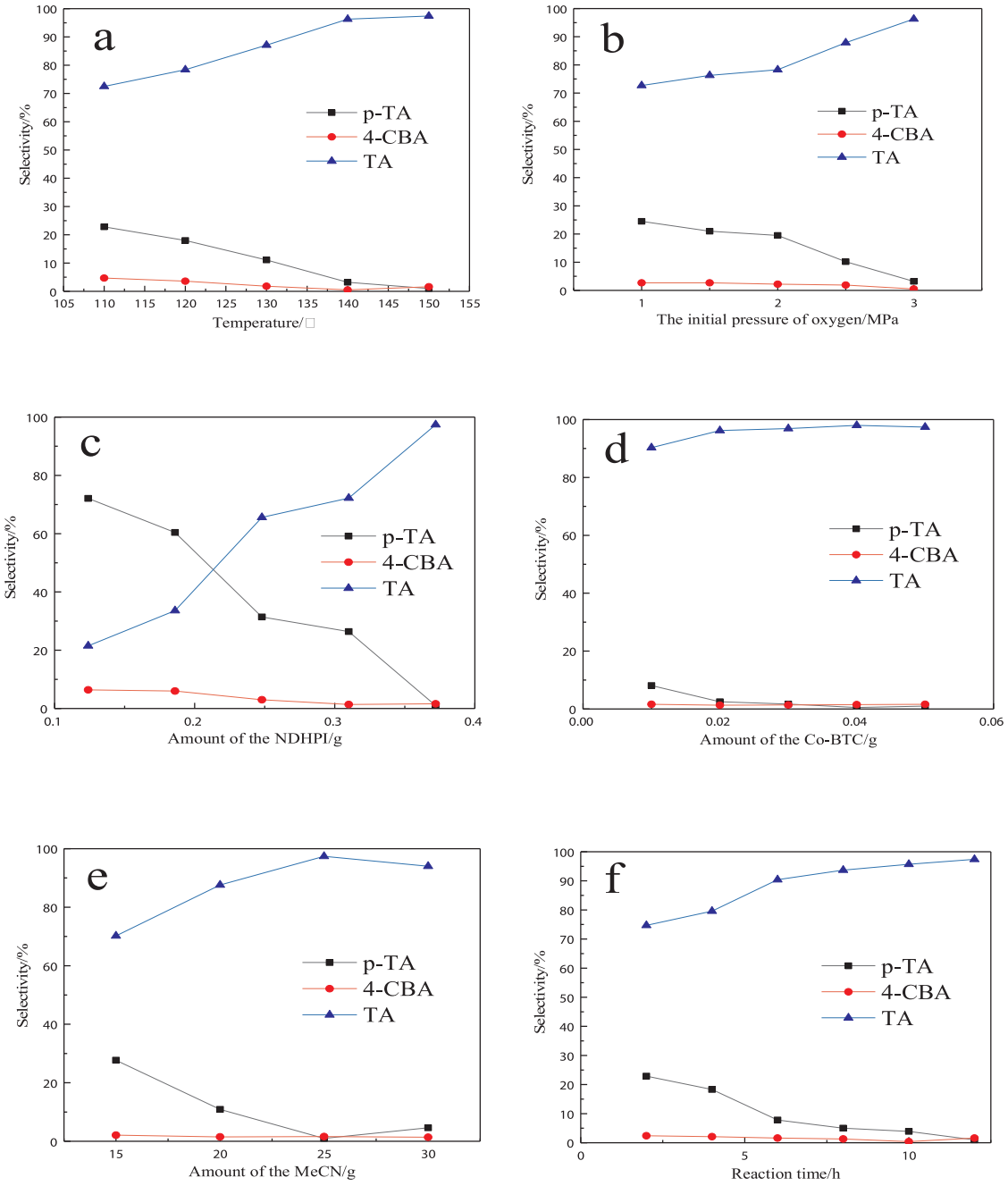

Fig. 6. Reaction parameter study. The conversion of PX was 100 % in Fig. 6a–f. The operating conditions of reactions **a-f** were varied as follows: NDHPI (0.372 g), Co-BTC (0.05 g), PX (0.54 g), MeCN (25 g), O_2 (3.0 MPa), 150 °C, 12 h.

the main peaks and the accompanying peaks are 5.8 eV and 5 eV, respectively. The energy gap between the main peak of Co2p and the satellite peak serves as an important criterion for judging the oxidation state of the Co cation. It is generally accepted that the energy gap for a Co(II) cation is about 5 − 6 eV, whereas that for a Co(III) cation is 9 − 10 eV. Therefore, the cobalt in Co-BTC is Co(II). Fig. 5 shows SEM images of the prepared Co-BTC. It can be seen that the surface of the synthesized Co-BTC was extremely irregular, with many gaps. This is consistent with the characterization from the N_2 sorption isotherm.

3.2. Study of catalytic performance

Table 1 shows the performance of Co-BTC in combination with NDHPI for the catalytic oxidation of P X . It is well known that PX is difficult to oxidize without a catalyst. Reactions 1 and 2 used NDHPI and Co-BTC alone as catalysts, respectively, and when the reactions were attempted at 100 °C for 12 h, no product was detected. Only when Co-BTC was used in combination with NDHPI was the product detected. The conversion of PX was 57 %, and the selectivity for the main product *p*-TA was 89.4 %. We then increased the reaction temperature to 150 °C, and the amounts of reactant and solvent were shown as conditions **b** in Reactions 5, 6, and 7. Under conditions **b**, PX was oxidized when NDHPI and Co-BTC were used alone, and the conversion rates were 93.5 % and 3.1 %, respectively. When they were used together as co-catalysts (Reaction 6), conversion of PX reached 100 %, and the selectivity for TA reached 96.2 %. In Reactions 6 and 7, under otherwise identical reaction conditions, we compared Co-BTC and $Co(OAc)_2{\cdot}4H_2O$ with the same cobalt content, and found that the selectivity for TA was higher when Co-BTC was used.

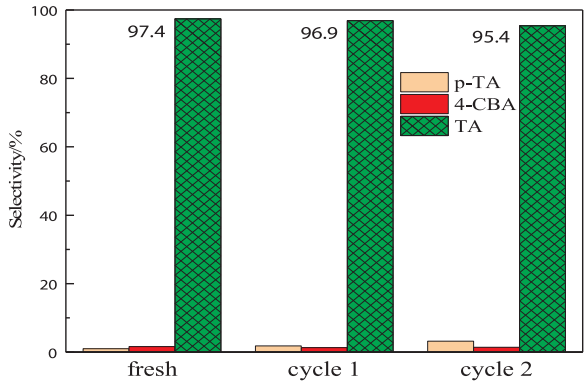

Fig. 7. Reusability study of Co-BTC catalyst for PX oxidation. The conversion of PX was 100 %. Reaction carried out at 150 °C for 12 h, 0.54 g PX, 0.372 g NDHPI, 0.05 g Co-BTC, 25 g MeCN, 3.0 MPa O_2.

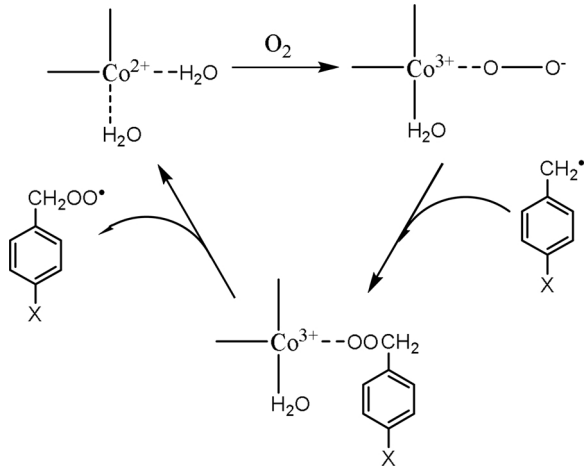

Scheme 2. Reaction mechanism of Co-BTC catalyst for *p*-methyl benzyl radical oxidation. X = CH_3, COOH.

3.3. Optimization of the reaction parameters

Fig. 6 shows an optimization of the reaction conditions for the oxidation of PX catalyzed by NDHPI and Co-BTC. The conversions of PX were 100 % in Fig. 6a–f. It can be seen from Fig. 6a and b that higher temperature and oxygen pressure are favorable for obtaining TA with high selectivity. In Fig. 6c and d, it is evident that the use of NDHPI as the main catalyst requires a large amount, which may be due to the self-decomposition of nitrogen-oxygen radicals by NDHPI during the reaction, as mentioned in the literature [6,45,47]. Conversely, the amount of Co-BTC required is extremely small; a loading of 0.08 wt% or more in the reaction mixture is sufficient to obtain a good effect. Fig. 6e shows that the reaction requires a suitable solvent ratio. In the 100 mL reactor, 25 g of MeCN and 0.54 g of PX gave a suitable ratio. Fig. 6f shows the relationship between reaction time and the selectivity for TA. The selectivity for TA reached 90 % at 6 h, but a further 6 h was needed to raise it from 90 % to 97 %. This may be attributed to the low content of *p*-TA.

3.4. Reusability study

We investigated the stability of Co-BTC in the oxidation of PX. When the reaction was complete, the solid product was dissolved in DMSO, and Co-BTC was separated by centrifugation. The isolated Co-BTC was washed three times with DMSO, three times with ethanol, and then vacuum-dried at 80 °C for 12 h for the next reaction. We performed two reuses and found that the performance of the catalyst was almost unchanged, as shown in Fig. 7. The first recovered catalysts were characterized by XRD and SEM, and the results are shown in Figs. 2 and 5. The diffraction peak of Co-BTC-cycle 1 showed little change compared to the fresh catalyst. SEM images showed that the catalyst was nearly spherical before and after the reaction.

3.5. Reaction mechanism

The oxidation of PX to TA is a very important hydrocarbon oxidation process, which is generally considered to follow a mechanism of hydrocarbon radical oxidation [5], and has to overcome the barriers associated with the following three steps:

$$CH_3(C_6H_4)CH_3 + \text{initiator} \rightarrow CH_3(C_6H_4)CH_2\blacksquare + \text{H-initiator} \quad (1)$$

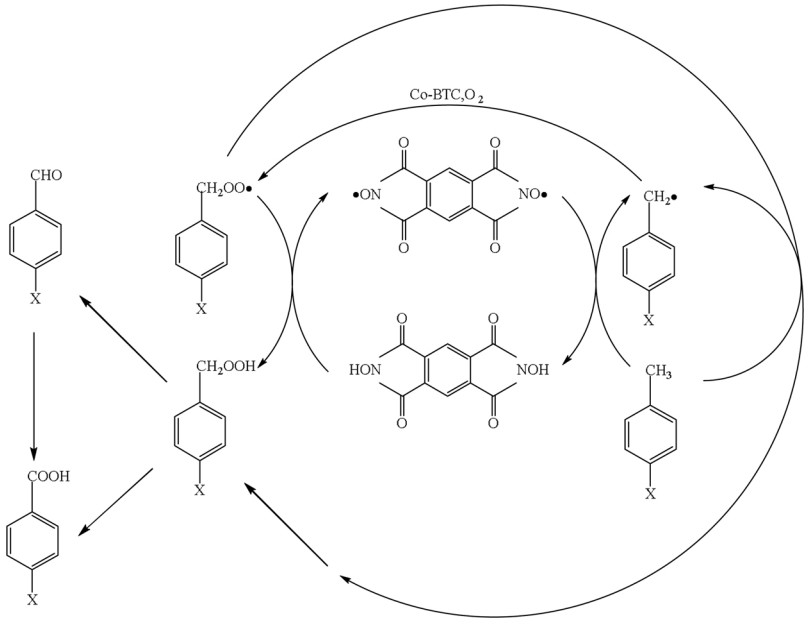

Scheme 3. Proposed reaction mechanism for the Co-BTC/NDHPI-catalyzed oxidation of PX. X = CH_3, COOH.

$$CH_3(C_6H_4)CH_2\blacksquare + O_2 \rightarrow CH_3(C_6H_4)CH_2OO\blacksquare \quad (2)$$

$$HOOC(C_6H_4)CH_3 + \text{initiator} \rightarrow HOOC(C_6H_4)CH_3\blacksquare + \text{H-initiator} \quad (3)$$

Eq. (1) is a common requirement in the oxidation of hydrocarbons. However, the oxidation of PX involves requirements that do not arise in general hydrocarbon oxidation (expressed by Eqs. (2) and (3)). Firstly, PX undergoes the process according to Eq. (1) to afford a *p*-methyl benzyl radical, which is strongly resonance-stabilized. According to Eq. (2), the peroxy *p*-methyl benzyl radical is produced. In this intermediate, the free electrons are separated from the ring double-bond conjugated system, and the radicals cannot form any resonance hybrids. Hence, it is destabilized, and the equilibrium of Eq. (2) is shifted towards the *p*-methyl benzyl radical. Therefore, the methyl groups of *p*-xylene are difficult to oxidize.

The oxidation of *p*-TA is even more difficult, because the carboxyl group is an electron-withdrawing group, as opposed to the initially oxidized electron-donating methyl group. Hence, electrons in the benzene ring are attracted to the carboxyl group, making it difficult for the methyl group in *p*-TA to generate a structurally stable CH_2 group by resonance. The presence of the carboxyl group attracts electrons and enhances the strength of the C—H bonds in the methyl group of *p*-TA [5].

NHPI and its derivatives are excellent initiators that can easily capture protons from alkyl groups, and they have received much attention in academia and industry. In the PX oxidation process, we used NDHPI as an initiator, the main function of which is to facilitate the processes described by Eqs. (1) and (3), generating hydrocarbon radicals that can react with oxygen.

The process according to Eq. (2) is difficult to achieve due to the antioxidant action of the *p*-methyl benzyl radical. To facilitate this step, we used Co-BTC as a catalyst. First, Co(II) on the surface of the catalyst coordinated by adsorbed oxygen is oxidized to Co(III). The molecular oxygen withdraws an electron from Co(II) to form O_2^- and Co(III), the *p*-methyl benzyl radical combines with O_2^-, the final Co(III)—O bond is broken, Co(III) is reduced to Co(II), and a peroxy *p*-methyl benzyl radical is formed. The process according to Eq. (2) is completed, as shown in Scheme 2. Saracco et al. [46] studied the adsorption of oxygen by Co-ZIF-67. They surmised that most of the cobalt in Co-ZIF-67 did not participate in the reaction with oxygen, with only the coordinatively unsaturated cobalt at the surface being involved. We believe that our non-porous synthesized Co-BTC undergoes a similar process.

We designed experiments to study the mechanism of the synergistic Co-BTC/NDHPI-catalyzed oxidation of PX. In Reactions 1, 2, and 3 in Table 1, when NDHPI is used alone, although it has strong hydrogen-abstracting ability, PX can only be converted into *p*-methyl benzyl radical. Due to the resistance to oxidation, Eq. (2) is difficult to accomplish. When Co-BTC is used alone, it lacks hydrogen-scavenging ability, and at 100 °C, the CH bonds of the methyl group are difficult to cleave to form hydrocarbon radicals. Only when these components are used together as co-catalysts can PX be readily oxidized at 100 °C.

Based on the above, we speculate that the mechanism of the Co-BTC/NDHPI-catalyzed oxidation of PX to TA may be as shown in Scheme 3. The main role of NDHPI is to capture hydrogen from the methyl group, while Co-BTC catalyzes the oxidation of hydrocarbon radicals to hydrocarbon peroxy radicals.

4. Conclusions

A new cobalt-based metal-organic framework, Co-BTC, with a non-porous structure, has been synthesized. It has been used in combination with NDHPI to co-catalyze the oxidation of PX to TA. Under optimized conditions of 150 °C in acetonitrile, the conversion rate of PX reached 100 % and the selectivity for TA exceeded 97 %. Co-BTC can be recycled and reused, retaining its structure and activity. Compared to existing procedures, the lower temperature and avoidance of corrosive bromine and acetic acid make this a green, mild reaction process. A reaction mechanism has been proposed, whereby the main function of NDHPI is to extract hydrogen from the two methyl groups of PX, whilst the main function of Co-BTC is to promote the reaction of hydrocarbon radicals with oxygen to form hydrocarbon peroxy radicals.

CRediT authorship contribution statement

Luo Xu: Investigation, Formal analysis, Visualization, Writing - original draft.

Dawei Chen: Purchase of raw materials and equipment.

Haoran Jiang: Characterization of the catalyst.

Xia Yuan: Conceptualization, Writing - review & editing, Project administration, Funding acquisition.

Declaration of Competing Interest

The authors declare that they have no known competing financial interests or personal relationships that could have appeared to influence the work reported in this paper.

Acknowledgments

This study was financially supported by the National Natural Science Foundation of China (No. 21776237).

References

[1] I. Hermans, J. Peeters, P.A. Jacobs, J. Org. Chem. 72 (2007) 3057–3064.
[2] H.S. Blanchard, J. Am. Chem. Soc. 81 (1959) 4548–4552.
[3] I. Hermans, T.L. Nguyen, P.A. Jacobs, J. Peeters, ChemPhysChem 4 (2005) 637–645.
[4] I. Hermans, P.A. Jacobs, J. Peeters, Chem. Eur. J. 16 (2006) 4229–4240.
[5] R.A.F. Tomás, J.C.M. Bordado, J.F.P. Gomes, Chem. Rev. 113 (2013) 7421–7469.
[6] F. Recupero, C. Punta, Chem. Rev. 107 (2007) 3800–3842.
[7] Y. Tashiro, T. Iwahama, S. Sakaguchi, Y. Ishii, Adv. Synth. Catal. 343 (2001) 220–225.
[8] N. Koshino, B. Saha, J.H. Espenson, J. Org. Chem. 68 (2003) 9364–9370.
[9] C.R. Jacob, S.P. Varkey, P. Ratnasamy, Appl. Catal. A Gen. 182 (1999) 91–96.
[10] S.A. Chavan, D. Srinivas, P. Ratnasamy, J. Catal. 204 (2001) 409–419.
[11] K. Deori, D. Gupta, B. Saha, S. Deka, ACS Catal. 4 (2014) 3169–3179.
[12] Q. Jiang, H.Y. Hu, C.C. Guo, Q. Liu, J.X. Song, Q.H. Li, J. Porphyrins Phthalocyanines 11 (2007) 524–530.
[13] T. He, X.B. Xu, B. Ni, H.F. Lin, C.Z. Li, W.P. Hu, X. Wang, Angew. Chem. 130 (2018) 10305–10309.
[14] F. Shi, M. Hammoud, L.T. Thompson, Appl. Catal. B Environ. 103 (2011) 261–265.
[15] C. Montoro, F. Linares, E.Q. Procopio, I. Senkovska, S. Kaskel, S. Galli, N. Masciocchi, E. Barea, J.A.R. Navarro, J. Am. Chem. Soc. 133 (2011) 11888–11891.
[16] P.Z. Li, X.J. Wang, Y.X. Li, Q. Zhang, R. He, D. Tan, W.Q. Lim, R. Ganguly, Yanli Zhao, Microporous Mesoporous Mater. 176 (2013) 194–198.
[17] C.M. Lu, J. Liu, K.F. Xiao, A.T. Harris, Chem. Eng. J. 156 (2010) 465–470.
[18] Y.J. Ma, Z.M. Wang, X.F. Xu, J.Y. Wang, Chin. J. Catal. 38 (2017) 1956–1969.
[19] J.P. Li, S.J. Cheng, Q. Zhao, P.P. Long, J.X. Dong, Int. J. Hydrogen Energy 34 (2009) 1377–1382.
[20] P.D. Hu, M.C. Long, Appl. Catal. B 181 (2016) 103–117.
[21] R.J. Kuppler, D.J. Timmons, Q.R. Fang, J.R. Li, T.A. Makal, M.D. Young, D.Q. Yuan, D. Zhao, W.J. Zhuang, H.C. Zhou, Coord. Chem. Rev. 253 (2009) 3042–3066.
[22] K.K. Gangu, S. Maddila, S.B. Mukkamala, S.B. Jonnalagadda, Inorganica Chim. Acta 446 (2016) 61–74.
[23] M. Cheng, C. Lai, Y. Liu, G.M. Zeng, D.L. Huang, C. Zhang, L. Qin, L. Hu, C.Y. Zhou, W.P. Xiong, Coord. Chem. Rev. 368 (2018) 80–92.
[24] Z.G. Sun, G. Li, L.P. Liu, H.O. Liu, Catal. Commun. 27 (2012) 200–205.
[25] A.A. Alshehri, A.M. Alhanash, M. Eissa, M.S. Hamdy, Appl. Catal. A Gen. 554 (2018) 71–79.
[26] T. Zhang, Y.Q. Hu, T. Han, Y.Q. Zhai, Y.Z. Zheng, ACS Appl. Mater. Interfaces 10 (2018) 15786–15792.
[27] A. Dhakshinamoorthy, A.M. Asiri, H. Garcia, Chem. Eur. J. 22 (2016) 8012–8024.
[28] N. Nagarjun, A. Dhakshinamoorthy, New J. Chem. 43 (2019) 18702–18712.
[29] H. Noh, Y.X. Cui, A.W. Peters, D.R. Pahls, M.A. Ortuño, N.A. Vermeulen, C.J. Cramer, L. Gagliardi, J.T. Hupp, O.K. Farha, J. Am. Chem. Soc. 138 (2016) 14720–14726.
[30] H.T.D. Nguyen, Y.B.N. Tran, H.N. Nguyen, T.C. Nguyen, F. Gándara, P.T.K. Nguyen, Inorg. Chem. 57 (2018) 13772–13782.
[31] J.W. Brown, Q.T. Nguyen, T. Otto, N.N. Jarenwattananon, S. Glöggler, L.S. Bouchard, Catal. Commun. 59 (2015) 50–54.
[32] Y.Y. Ma, H.Y. Peng, J.N. Liu, Y.H. Wang, X.L. Hao, X.J. Feng, S.U. Khan, H.Q. Tan,

Y.G. Li, Inorg. Chem. 57 (2018) 4109–4116.
[33] A. Dhakshinamoorthy, A.M. Asiri, H. Garcia, Chem. Commun. 53 (2017) 10851–10869.
[34] X. Shu, Y. Yu, Y. Jiang, Y. Luan, D. Ramella, Appl. Organoment. Chem. 31 (2017) 1–8.
[35] T.W. Goh, C.X. Xiao, R.V. Maligal-Ganesh, X.L. Li, W.Y. Huang, Chem. Eng. Sci. 124 (2015) 45–51.
[36] Y. Li, M.Z. Wu, D.M. Chen, L. Jiang, J. He, Z.H. Luo, W. Wang, J.Q. Wang, Mol. Catal. 477 (2019) 110542.
[37] O.M. Yaghi, H.L. Li, T.L. Groy, J. Am. Chem. Soc. 118 (1996) 9096–9101.
[38] L. Xu, P.C. He, D.W. Chen, X. Yuan, Petrochem. Technol. (in China) 47 (2018) 861–866.
[39] H.X. Li, J.Q. Wan, Y.W. Ma, Y. Wang, X. Chen, Z.Y. Guan, J. Hazard. Mater. 318 (2016) 154–163.
[40] C. Li, X.B. Lou, M. Shen, X.S. Hu, Z. Guo, Y. Wang, B.W. Hu, Q. Chen, ACS Appl. Mater. Interfaces 8 (2016) 15352–15360.
[41] D.H. Ge, J. Peng, G.L. Qu, H.B. Geng, Y.Y. Deng, J.J. Wu, X.Q. Cao, J.W. Zheng, H.W. Gu, New J. Chem. 40 (2016) 9238–9244.
[42] D.H. Ge, G.L. Qu, X.M. Li, K.M. Geng, X.Q. Cao, H.W. Gu, New J. Chem. 40 (2016) 5531–5536.
[43] F. Luo, Y.X. Che, J.M. Zheng, Eur. J. Inorg. Chem. 2007 (2007) 3906–3910.
[44] K. Liu, Z.R. Shen, Y. Li, S.D. Han, T.L. Hu, D.S. Zhang, X.H. Bu, W.J. Ruan, Sci. Rep. 4 (2014) 1–7.
[45] R. Amorati, M. Lucarini, V.E. Mugnaini, G.F. Pedulli, F. Minisci, F. Recupero, F. Fontana, P. Astolfi, L. Greci, J. Org. Chem. 68 (2003) 1747–1754.
[46] C. Ueda, M. Noyama, H. Ohmori, M. Masui, Chem. Pharm. Bull. 35 (1987) 1372–1377.
[47] G. Saracco, S. Vankova, C. Pagliano, B. Bonelli, E. Garrone, Phys. Chem. Chem. Phys. 16 (2014) 6139–6145.